



AD 717553

AD

TECHNICAL REPORT

WVT-7012

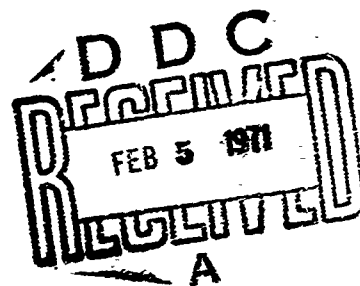
SUSCEPTIBILITY OF GUN STEELS TO STRESS CORROSION CRACKING

BY

VITO J. COLANGELO

AND

MARTIN S. FERGUSON



This document has been approved
for public release and sale; its
distribution is unlimited

NOVEMBER 1970

BENET R&E LABORATORIES

WATERVLIET ARSENAL

WATERVLIET—NEW YORK

AMCNS No. 4930.16.6691

DA Project No. 66661

Reproduced by
NATIONAL TECHNICAL
INFORMATION SERVICE
Springfield, Va 22151

49

TABLE OF CONTENTS

	PAGE
Abstract	1
Glossary	2
Acknowledgment	3
Introduction	4
Theories of Stress Corrosion Cracking	5
Preferential Path Theories	7
Mechanical Damage Theories	9
Procedure	11
Results	18
Relative Susceptibility of Gun Tubes	19
Effects of Environment	20
Effect of Yield Strength	21
Discussion	23
Conclusions	35
References	37
DD Form 1473	

ILLUSTRATIONS

		PAGE
Figure 1	Geometry of Cantilever Beam Specimen	13
Figure 2	Schematic of Pre-cracking Machine	14
Figure 3	Schematic Drawing of Fatigue-cracked Cantilever Beam Test Apparatus	16
Figure 4	Susceptibility of As-received Specimens to Cracking in 3% Oxygenated NaCl	22
Figure 5	Effect of Environment on Fracture Time, Tube 7, 186 ksi YS	22
Figure 6	Effect of Yield Strength on Fracture Time, Heat-treated Tube 1100 in Distilled H ₂ O	25
Figure 7	Intergranular Stress Corrosion at Crack Tip of Tube 7 in Aqueous Salt Environment (1000X Nital Etch)	25
Figure 8	Macro Photo of Failure Surfaces of Gun Tubes 1382 and 7 showing Thumbnail Corrosion Markings	26,27
Figure 9	Curve Illustrating Effect of Yield Strength on Crack Growth	31
Figure 10	Effect of Yield Strength on Crack Growth - Tube 1100 in 3% NaCl - Stress Intensity Factor of 50 ksi√Inch	31
Figure 11	Fractograph Showing Intergranular Stress Corrosion Crack (3200X)	33
Figure 12	Fractograph Showing H ₂ Charge Brittle Fracture (3200X)	34

TABLES

I	Mechanical Properties of Specimens and As-received Tubes	17
II	Nominal Composition (Weight %) Gun Steel vs. 4340 Steel	19
III	Fracture of Gun Steel in Oxygenated 3.0% Sodium Chloride	20
IV	Effect of Environment on Fracture of Gun Steel, Tube 7	21
V	Effect of Yield Strength of Gun Steel on SCC in Distilled Water	23

SUSCEPTIBILITY OF GUN STEELS TO STRESS CORROSION CRACKING

ABSTRACT

Cross-Reference Data

Precracked cantilever beam specimens extracted from specific gun tubes were subjected to a constant load in various environments to determine fracture times. Specimens exhibited stress corrosion susceptibility in 3% NaCl, distilled water and 100% RH air, with 3% NaCl being the most degrading environment. Variations in susceptibility appeared on a tube to tube basis and were related to the temper embrittled condition of the tube.

Stress-corrosion

High strength
steels

Hydrogen-
embrittlement

Temper
embrittlement

Precracked bend
specimens

Additional tests in distilled water, varying yield strength material, showed that fracture time was decreased and crack growth rates increased as the yield strength was increased.

Fracture
mechanics

GLOSSARY

- K, K_I - Stress intensity factor; the subscript I denotes opening mode of crack extension.
- K_{Ic} - The plane strain fracture toughness determined by chevron notch slow bend test with three-point loading of specimen dimensions 1 x 2 x 8".
- K_{Ix}, K_{Ii} - Stress intensity loading factors; x denotes dry fracture by loading specimen to failure; i denotes initial stress intensity factor in loaded specimens.
- K_{Isc} - The K_{Ii} value which will not produce failure in the observation period and below which there appears to be no further susceptibility to stress corrosion.
- YS - The yield strength value of 0.1% strain offset.
- R_c - Hardness value, Rockwell C scale.
- C_v - Charpy impact strength in ft-lb @ -40°F.
- %RA - % reduction in area at tensile failure.
- EFC - Effective full charge rounds.
- a_c - Critical crack depth; the depth at which fast fracture is initiated.
- 100% RH - Saturated humidity at room temperature (specimen exposed over distilled water).

ACKNOWLEDGMENTS

The authors acknowledge, with thanks, helpful discussions with Mr.
T. M. Pochily.

SUSCEPTIBILITY OF A GUN STEEL TO STRESS CORROSION CRACKING

INTRODUCTION

The problem of premature failure of alloys by stress corrosion has long been recognized. At least fifty years ago, the ASTM held discussions on the corrosion cracking of brass⁴.

Interaction of mechanical tensile stresses in a chemically aggressive environment causes cracking that is impossible to predict by independent mechanical or corrosion testing.

Four basic requirements are necessary to cause stress corrosion cracking: a susceptible alloy, an aggressive environment, applied or residual stresses and time.

The purpose of this study was to investigate the parameters affecting stress corrosion cracking in a gun tube material. There were a number of questions to be resolved: whether this gun steel (4337 modified) is susceptible to stress corrosion, the nature of environments encountered that may be considered aggressive and the rate of attack as influenced by yield strength levels. The possible role of stress corrosion^{1,2,3} in untimely field failure of gun tubes is also a consideration of this investigation.

THEORIES OF STRESS CORROSION CRACKING

Stress corrosion has been observed in many diverse materials and environments. The current literature contains numerous references to fracture of titanium, brass, aluminum, magnesium and various steel alloys⁵⁻¹³. With such a variety of distinctly different conditions of

fracture, it is difficult to find common features. In work by Hoar¹⁴ and Hines¹⁵, Hines¹⁶, and Parkins¹⁶, the following characteristics consistent with this type of fracture have been observed, however:

1. There must be simultaneous action of stress and corrosion; alternate application of stress and corrosion will not produce similar results. The fracture surfaces are macroscopically brittle, with little signs of ductile tearing.

2. The induction period necessary to produce crack initiation and pitting is relatively long compared with actual crack propagation. Stress plays little part in the induction period; corrosion is the primary driving force. Embrittlement of the region surrounding the crack tip may also be a significant factor in the induction process.

3. The mode of cracking can be intergranular or transgranular, but is predominately one or the other in any test. No generalizations can be made regarding the effect of changes in heat treatment or compositions on mode, but one type of cracking appears to occur more readily for each particular alloy.

4. The rate of advance is quite rapid at the crack tip; much less at the walls. The crack propagation process appears to be self-stimulating with the much larger rate being sustained only at the advancing crack tip.

5. Conditions for cracking are specific as to alloy and environment. Specific ions are usually necessary to promote cracking conditions. Although many environments may produce similar corrosion rates, susceptibility of different metals to stress corrosion may be

widely divergent. Certain corrodents giving relatively violent reaction with an alloy do not cause cracking. The question is thus raised of the contributing interaction of corrodent anions to failure.

Tensile stress at the corroding surface is essential to stress corrosion cracking. These tensile stresses may be residual or applied. Both are detrimental to service life and the degree of degradation is dependent on the magnitude of stresses. Residual stresses may be more of a problem, however, since they are frequently concealed and neglected in designing for safety factor of the component¹⁷. These internally induced stresses arise from processing differences such as non-uniform deformation during cold working, or unequal cooling rates from annealing temperatures. Other built-in stresses include those induced by press or shrink fits and other fastened deformations such as rivets or bolts.

The many theories that have been advanced to explain stress corrosion cracking generally fall into one of two mechanisms: (1) one in which electrochemical processes account for crack propagation by means of dissolution along preferential paths, and (2) an alternating step-fracture sequence where mechanical fracture is triggered by corrosion. To reach the characteristic high rate of propagation, a means must be found to satisfy: either a type of corrosion process capable of high penetration rates in the region of the crack tip, or a means whereby corrosion can produce localized embrittlement and lead to intermittent mechanical fracture.

PREFERENTIAL PATH THEORIES

An early theory proposed by L. H. Dix¹⁸ suggested that susceptible paths exist and corrosion follows under the action of tensile stresses perpendicular to these paths. This mechanism allows corrosion to follow a path held open by stresses and is quite suitable to explain intergranular attack along grain boundaries which are more reactive to corrosion. The relatively high rates of crack propagation, caused solely by grain boundary differences, are difficult to visualize.

The feature most common to recent theories is the attempt to explain the very high and localized attack of metal at the tip of the crack. The difference in current density between the crack tip and walls has been linked to the highly localized attack at the tip. The elastic strain energy and plastically strained material at the crack tip may account for some of the concentrated attack if supplemented by other factors responsible for high current density.

Several dislocation theories have been proposed to explain fracture observations. Swann and Pickering¹⁹ have deduced that moving dislocations transport solute atoms to the free surface of the metal. Movement of these atoms to active slip planes, where a high density of dislocations is concentrated, produces the chemical inhomogeneity necessary to initiate and propagate stress corrosion cracking. Observation of the serrated type stress-strain curve (Portevin-LeChatelier effect) associated with intermittent plastic flow indicates that solute migration does occur with moving dislocations. Preferential corrosive attack²⁰ of components is a prerequisite causing faults that fracture mechanically. Studies have been made by Hines and Hugill²¹ to determine metallographically whether cracking has occurred electrochemically or mechanically, but have not been conclusive to date.

Varying alloy compositions have exhibited a marked difference in susceptibility to stress corrosion. Graf²² has advanced the theory that susceptibility should pass through a maximum as the concentration of a more noble alloying element is increased. Segregation of the alloying elements at grain boundaries, or separation from solution, establishes cathodic sites which accelerate attack at adjacent anodic areas. At higher alloying compositions the process of dissolution does not occur, and continuous paths in the more active metal no longer exist. Of particular significance to stainless steels is recent work by Copson²³ studying effects of nickel and chromium alloying. The matrix iron material is much more electrochemically active than either alloy; and susceptibility increases to a maximum at about 10% nickel, then decreases

as predicted by Graf. Copson also points out the fallacy of relying on "stable" protective films in steels. When such films are ruptured by highly corrosive environments such as ferric chloride solution, subsequent failure is quite rapid.

In apparent conflict with the previously mentioned electrochemical theory are studies of the wedging effect caused by buildup of corrosion products. Nielsen²⁴ has obtained excellent photomicrographs of filled microcracks in stainless steels where the volume of corrosion product, if unconstrained, would be twice that of the removed metal. Consequently, high stresses were generated. Pickering²⁵, et al, studied stainless steels in dilute chloride solutions at autoclave temperatures of 400°F. Pressures of 4000-7000 psi due to the corrosion products have been measured. Corrosion products identified include ferric and ferrous oxides, cubic chromium oxide and complex chrome-iron oxides.

MECHANICAL DAMAGE THEORIES

Heating²⁶ and Evans²⁷ have advanced theories to explain high crack propagation rates in terms of alternating mechanical and electrochemical stages. It is theorized that notches are produced by corrosion and a brittle fracture occurs along a mechanically weak path until an obstacle is reached. Crack propagation occurs by the repeated occurrence of this cycle. This theory is quite useful at grain boundaries where it is known that precipitates are anodic to the matrix material, and hence are susceptible corrosion sites²⁸. Logan^{29,30} has theorized that local yielding disrupts the polarized condition of surface oxide films to the extent that crack sides remain passive and the advancing crack

tip becomes active. The crack propagates if the strain at the tip ruptures the protective film at a higher rate than it can be repaired. Pour and Lines¹⁴ went a step further and speculates that this local yielding assisted in actual removal of cations from the metal lattice.

Mines^{31,32} has discussed the conditions necessary for electrochemical attack at a crack tip. He has postulated that an ohmic drop exists within the crack whereby the crack tip and surface exhibit markedly different corrosion rates.

Mechanical mechanisms, including embrittlement and stacking fault theories, have been advanced to explain cracking of normally ductile materials. Barnett and Troiano³³ have described the steps of hydrogen-induced static fatigue of high strength AISI 4340 steel. Under sustained load, the process is one of crack initiation and slow crack growth followed by cataclysmic brittle fracture. The stages were identified and followed using photographic and electrical resistance measurements. Kim and Loginow³⁴ have recently reported measurements of hydrogen concentration and permeability in a Ni-Cr-MO steel. A concept of hydrogen trapping was proposed to explain the higher concentration in steels of increasing yield strength, of the same composition. Evans³⁵ advanced an embrittlement theory in which hydrogen formed near the crack tip could diffuse into the highly strained crack tip and cause propagation of brittle fracture. Reduction of hydrogen ions at the crack tip is likely in light of the lower potential and higher acidity exhibited. Brown³⁶ has indeed reported pH and metal ion studies at the crack tip using liquid nitrogen to freeze the solution in a cracked specimen. This data is used to support the hydrogen embrittlement

theory for high strength steels. It must be noted, however, that hydrogen cannot be responsible in all cases since metal systems more electrochemically noble than the hydrogen potential also suffer stress cracking.

Further evidence in support of the alternating electrochemical-mechanical theory of crack propagation has recently been added by McEvily and Bond³⁷ and Logan, et al³⁸. The former work on brass contains excellent replica electron micrographs clearly showing discontinuous step-wise crack propagation. Rupture of the protective tarnish has been shown to concentrate the effects of environment. Subsequent work with aluminum, zinc and magnesium alloys showed similar results. Logan's³⁸ work with 321 stainless steels has produced electron micrographs showing the discontinuous process of fracture. It was theorized that the tendency of austenitic stainless steel to work harden produces increments too small to be detected by simple elongation measurements.

PROCEDURE

Many test specimen configurations have been proposed for environmental testing. For our use, it was necessary to choose one that would be representative of bulk gun steel material, yet also be small enough so that transverse specimens could be easily obtained from forgings and sections of fired gun tubes. Cantilever beam specimens of the type used by Brown³⁹ were modified for use in a dead weight loading rack. Size requirements for plane strain could not always be met from test materials available. Dimensions of the bent beam specimen are shown in figure 1. A sharp machine notch across the top face of the specimen

acts as a stress raiser to obviate the need for a long induction period to produce "natural" stress concentration points in the form of pits. Stress is further concentrated by eccentrically fatigue cracking in a precracking unit (figure 2) at low loading to "sharpen" the machine notch and extend the crack a nominal 20 to 30 thousandths inch deep. In such a sub-sized specimen, it becomes important to eliminate the effects of shear lips to minimize surface effects. Sharp side grooving is accomplished in the plane of proposed fracture to minimize these shear lips.

The rack used for dead weight loading is shown in figure 3 with stressed specimens in place. Essential features to be noted are: the stationary rack and timing clocks with pull-out switches to measure fracture time, the loading beam with dial indicator to detect opening movement, the specimen surrounded by polyethylene environmental chamber and the various weights supported from cantilever beam calculated to produce varying initial stress intensity factors at the root of specimen notch. The test is initiated by placing the precracked specimen into the apparatus shown and applying stress weights to it as a cantilever beam. This arrangement permits simple detection of crack opening initiation by observation of the change in dial indicator readings.

Environments extensively studied included distilled water, 100% relative humidity and 3.0% aqueous sodium chloride solution. Specimens tested in the 3.0% salt solution were also oxygen saturated by slowly bubbling the gas through the solution.

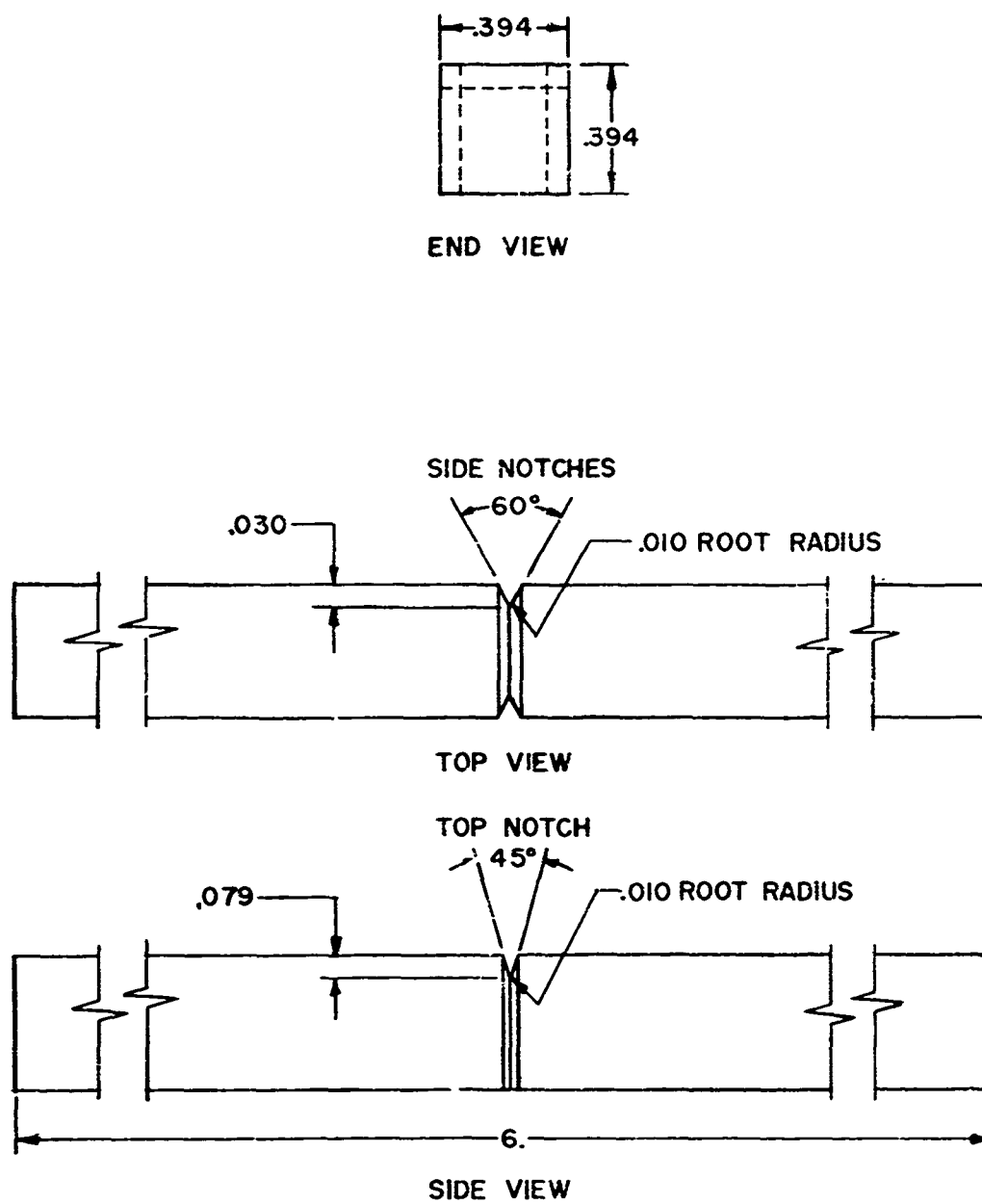


Figure 1. Geometry of cantilever beam specimen.

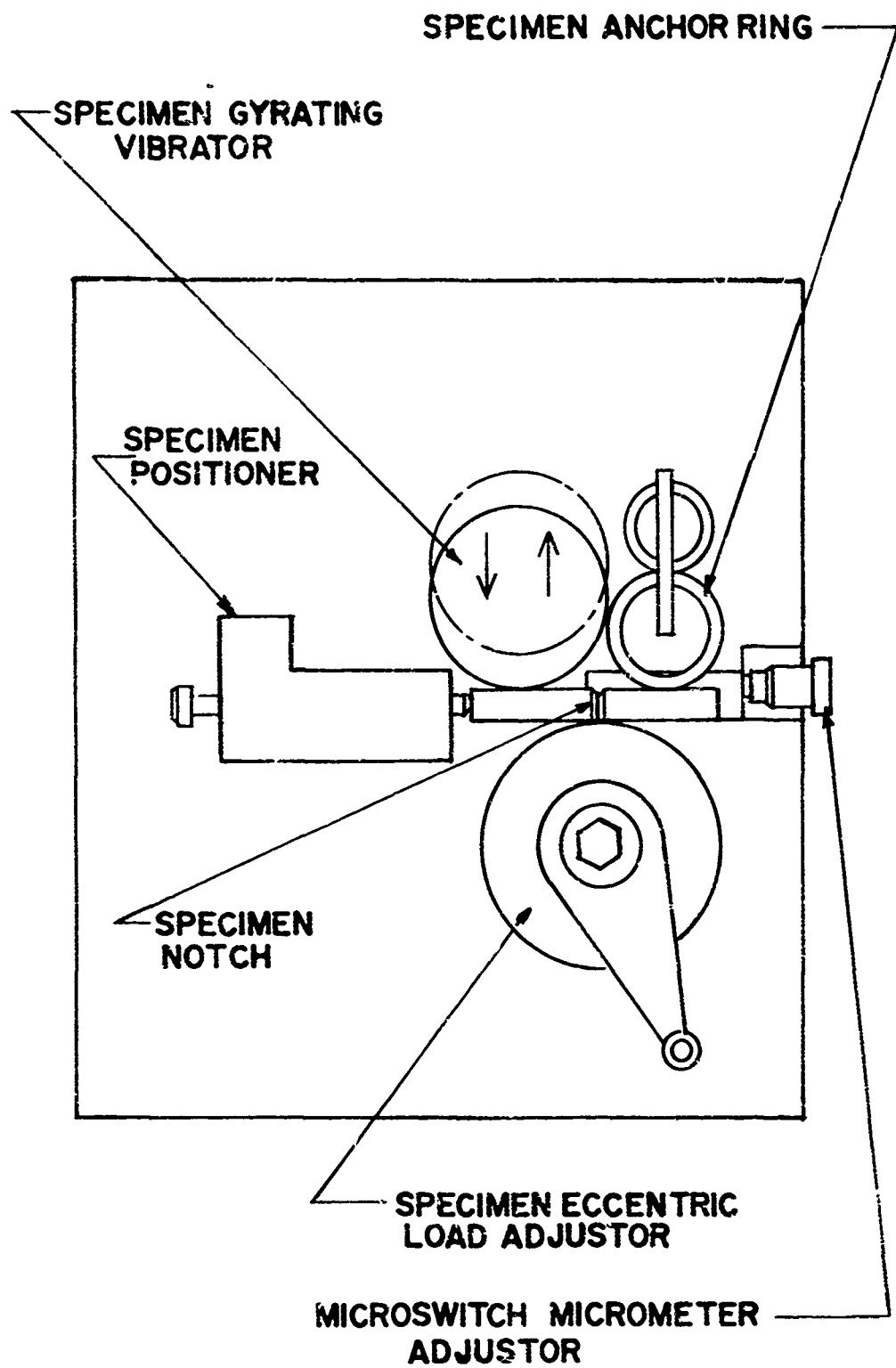


Figure 2. Schematic of pre-cracking machine.

Specimens were machined from various tube sections to study the susceptibility to stress corrosion cracking of representative materials in the "as received" condition. Further specimens from the least susceptible tube tested (tube 1100) were reheat treated to yield strengths varying from 142-205 ksi at 0.1% offset. Mechanical properties for all the tubes are tabulated in table I. Data shown for prepared specimens are mean values obtained from three tests.

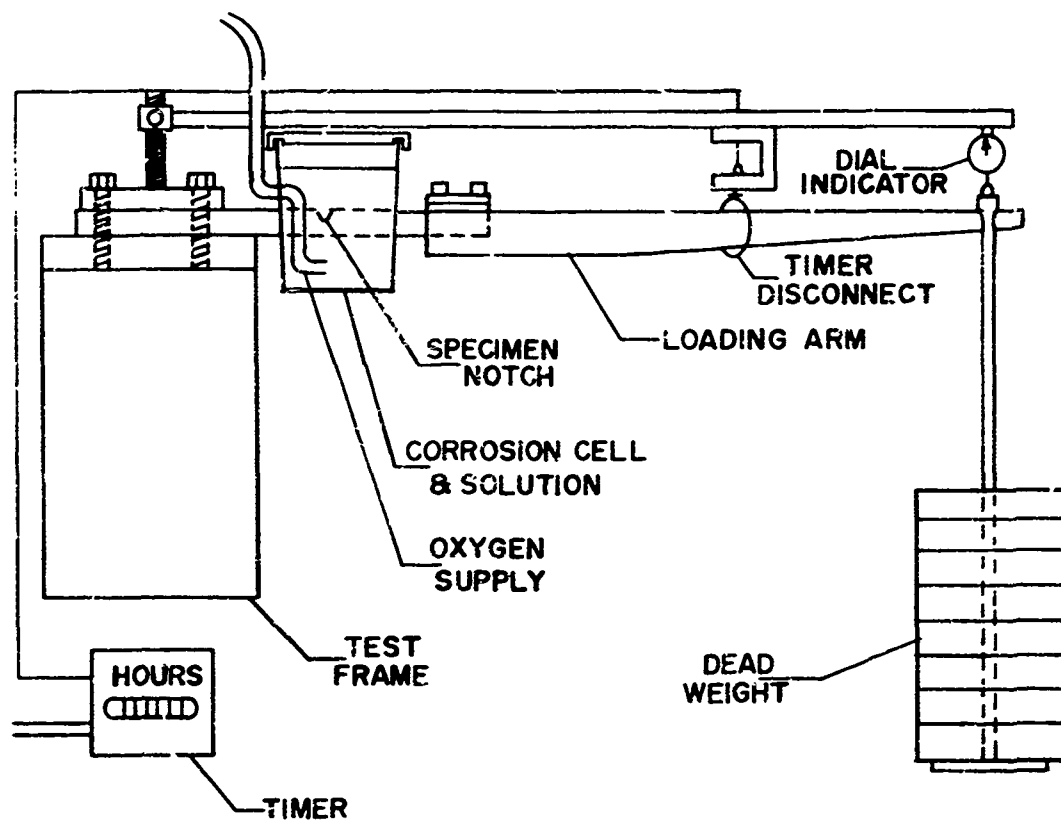


Figure 3. Schematic drawing of fatigue-cracked cantilever beam test apparatus.

TABLE I. MECHANICAL PROPERTIES OF SPECIMENS AND AS-RECEIVED TUBES

	Tube Serial Number	Specimens Prepared				Tube History	
		YS (ksi) 0.1% Offset	Hardness RC	Charpy (ft.lb) -40°F	% RA	Temperature °F	Total Cycles *
As Received	7	186	45	10.5	29	920	3325
	1382	185	45	10.6	21	915	1411
	1386	180	44	12.7	32	1000	4697
	1984	178	43	9.6	26	1040	5450
	1985	181	43	9.0	42	1040	6209
	1100	186	44	21.5	37	1036	7631
Heat	1100H	142	53	-	51	1175	-
Treated	1100D	200	49	-	25	500	-

*Reference 2

RESULTS

A preliminary estimate of the toughness of each group of specimens was obtained by loading a specimen stepwise to fracture in air. The stress intensity factor was calculated from equations of Bueckner⁴⁰, with refinements of Paris⁴¹ and corrections by Irwin, applied for face notching to give the relationship:

$$K_I = \frac{6M[f(a/h)]}{(b \cdot bn)^{1/2}(h-a)^{3/2}}$$

where K_I = stress intensity factor

M = bending moment

b = specimen width and bn is net width after side notching

h = specimen depth

a = crack length including fatigue extension

and $[f(a/h)]$ = function of a/h as tabulated in Kolfe, et al, (reference 43)

It must be pointed out that these initial loading fractures do not give valid K_{Ic} measurements as discussed by Kies, et al⁴². The K value for dry fracture on increasing load is designated K_{Ix} and merely gives a maximum loading stress intensity to be used as a measure for environmental testing. For this size specimen of high strength gun steel, the ratio of K_{Ix} to yield strength was such that valid K_{Ic} measurements could not be obtained. The procedure can still be used to compare results on the basis of nominal fracture stress by employing side grooving. These grooves prevent shear lip formation by developing a triaxial stress state at the fatigue crack. Consequently very little

deformation is produced in fracture. Further use is made of the equation in calculating the initial stress intensity factor, K_{Ii} , when loading the test specimen. With the specimen in place, the dial indicator reading is zeroed, then closely monitored for signs of crack opening. In the case of specimen failure, fracture times versus initial stress intensity K_{Ii} were recorded and plotted.

RELATIVE SUSCEPTIBILITY OF GUN TUBES

No data presently exists on the effect of stress corrosion, on gun steels of this type, though considerable data has been collected on 4340 steel, which is of similar composition as shown in table II.

TABLE II. NOMINAL COMPOSITION (WEIGHT %)
GUN STEEL VS. 4340 STEEL

		<u>C</u>	<u>Mn</u>	<u>Ni</u>	<u>Cr</u>	<u>Mo</u>	<u>Si</u>	<u>V</u>	<u>P</u>	<u>S</u>
Gunsteel Min.		.28	.70	2.75	.60	.30	.20	.10	-	-
4337V										Balance Fe
4337V	Max.	.34	1.00	3.50	1.00	.70	.35	.25	.025	.025
4340	Min.	.38	.60	1.65	.70	.20				
										Balance Fe
	Max.	.43	.80	2.00	.90	.30				

To assess susceptibility of as-received gun tubes to stress corrosion, specimens listed in table I were exposed to oxygenated 3.0% sodium chloride, an environment considered highly aggressive. The times to fracture under decreasing load conditions are shown below in table III. The graphical representation of figure 4 shows the range of data obtained, and clearly points out the increased degradation of tubes 7 and 1382.

TABLE III. FRACTURE OF GUN STEEL IN OXYGENATED
3.0% SODIUM CHLORIDE

Tube	K_{Ic}	K_{Ix} in air ksi $\sqrt{\text{inch}}$	K_{Ii} at Loading ksi $\sqrt{\text{inch}}$	% K_{Ii}/K_{Ix}	Hours to Fracture
7	117.5	109.1	90.5	83.0	2.7
			78.0	71.5	4.6
			63.7	58.3	8.0
			48.1	44.0	13.6
			32.1	29.4	688 *
1100	150	110.8	90.6	81.8	2.2
			84.9	76.6	3.0
			71.2	64.3	10.8
			54.6	49.2	40.2
			49.1	44.3	791 *
1382	98.2	94.5	84.6	89.5	0.3
			72.5	76.7	3.4
			66.3	70.2	7.2
			46.9	49.7	14.3
1386	106.0	104.5	83.6	80.0	2.5
			65.3	62.5	16.1
			51.6	49.4	18.0
			55.6	53.2	30.0
1984	-	103.9	89.3	86.0	0.2
			74.6	71.8	4.0
			59.7	57.5	10.8
			50.8	48.9	26.8
1985	-	103.6	85.1	82.2	2.1
			71.3	68.8	7.3
			60.6	58.5	15.9
			54.9	53.0	23.4
* Denotes no failure					

EFFECT OF ENVIRONMENT

Susceptibility was determined as previously described and further tests were run using the progressively less corrosive environments of distilled water and saturated humidity at room temperature.

One of the gun tubes, 7, that showed the black thumbnail markings at fatigued fracture surfaces, was chosen as material to study the effects of the other environments. Results are shown below in table IV and graphically in figure 5.

TABLE IV. EFFECT OF ENVIRONMENT ON FRACTURE
OF GUN STEEL, TUBE 7

Environment	K_{Ii}	% K_{Ii}/K_{Ix}	Hours to Fracture
Air (K_{Ix})	109.1	-	-
3.0% NaCl (Oxygenated)	78.0	71.5	4.6
	63.7	58.3	8.0
	48.1	44.0	13.6
	32.1	29.4	688 *
Distilled H_2O	90.8	83.2	8.1
	81.2	74.4	26.2
	64.5	59.1	72.2
	59.0	54.0	873
100% Humidity (Over distilled H_2O)	94.2	86.2	62.3
	91.1	83.5	76.9
	80.6	73.8	116
	72.5	66.5	221.7

*Denotes no failure

EFFECT OF YIELD STRENGTH

To study the effects of yield strength on stress corrosion attack, specimens from tube 1100, one of the tubes showing least susceptibility, were heat treated to various strengths as shown in

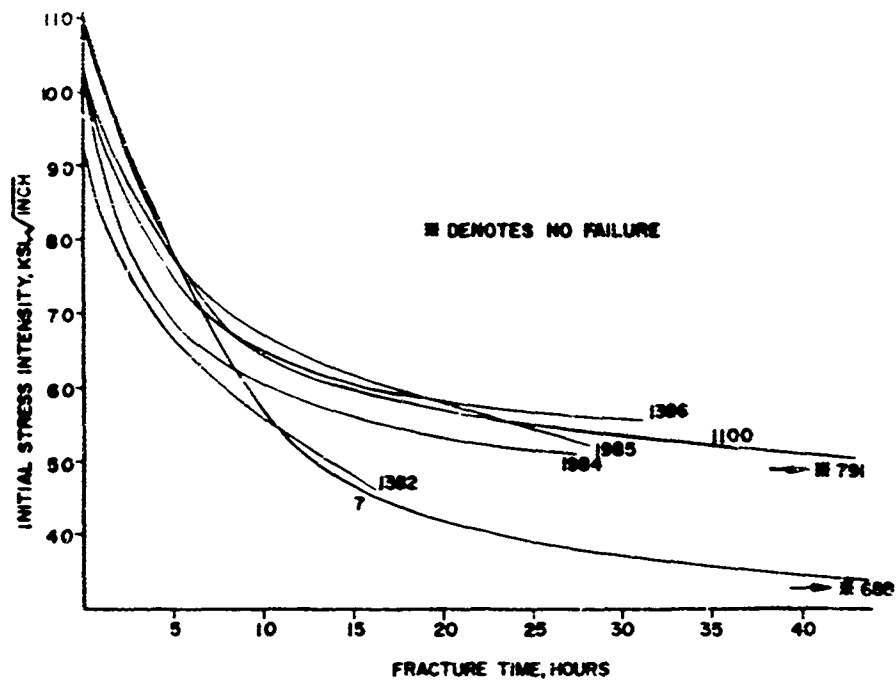


Figure 4. Susceptibility of as-received specimens to cracking in 3% oxygenated Na Cl.

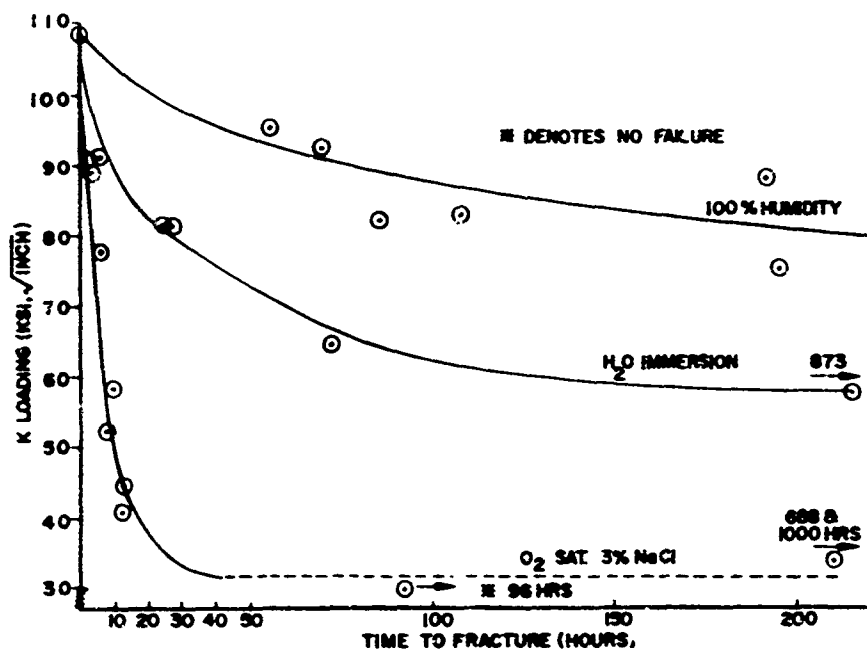


Figure 5. Effect of environment on fracture time, tube 7, 186 KSI YS.

table I. These steels were stressed in distilled water environment.

Tabulated below are fracture data shown in figure 6.

TABLE V. EFFECT OF YIELD STRENGTH OF GUN STEEL ON SCC
IN DISTILLED WATER

Y.S. (0.1% offset) ksi	$K_{I\bar{x}}$ in Air ksi $\sqrt{\text{inch}}$	$K_{I\bar{i}}$ at Loading ksi $\sqrt{\text{inch}}$	% $K_{I\bar{i}}/K_{I\bar{x}}$	Hours to Fracture	4340 Steel at Comparable Yield Strength $K_{I\bar{c}}$ (ksi $\sqrt{\text{inch}}$)**
142	104.2	91.5 95.6	87.6 91.6	554* 689	117
186	110.8	107.8 90.6 85.6 79.2	97.2 81.8 77.3 71.5	0.9 69.0 149.8 1167*	
200	88.7	75.8 58.1 47.2 41.9	85.5 65.5 53.1 47.3	1.2 20.7 80.4 814*	
* Denotes no failure ** 4340 data, Hays and Wessel ⁴⁶					

DISCUSSION

Stress corrosion damage is known to occur in 4340 steel and has been recently reported by Brown³⁹, Van Der Sluys⁴⁴ and Mulherin⁴⁵.

The initial question of whether the related gun steel alloy is similarly susceptible to stress corrosion damage is answered in table II and figure 4. These data show clearly that the gun steel, as represented by the several tubes shown, is suffering stress corrosion damage. As the level of the initial stress intensity factor $K_{I\bar{i}}$ is increased, the time to failure is decreased. The data also indicate a

difference in the response of the tubes tested. While all the tubes showed degradation as a result of immersion in the environment, tubes 7 and 1382 were affected most markedly, exhibiting a K_{ISCC} value of about 35 ksi $\sqrt{\text{inch}}$ as compared to an approximate value of 55 ksi $\sqrt{\text{inch}}$ for the other tubes tested. (The K_{ISCC} value is that value of the initial stress intensity factor which will not produce failure in the observation period and below which there appears to be no further degradation in properties.) This represents a reduction of about 65% from the K_{IX} value as compared to an average reduction of about 45% for the other tubes.

It is interesting to observe that if one compares the total cycles to failure (Zone 3 rounds + lab cycles), tubes 7 and 1382 rank lowest of the tubes shown. If one further compares the tempering temperatures for these tubes, tubes 7 and 1382 also show the lowest tempering temperature. These data indicate that these tubes were temper embrittled and support the contention by Davidson et al² that temper embrittlement increases stress corrosion susceptibility. With regard to fracture toughness, it is relevant to note that the K_{IX} values obtained agree very well with the K_{IC} values reported by Davidson although they are slightly lower in each case. In addition, the stress corrosion crack path for tube 7, as shown by figure 7, is intergranular. Tubes 7 (figure 8) and 1382 also show "black thumbnail" markings frequently associated with stress corrosion failures. These data support the premise that temper embrittlement increases the stress corrosion susceptibility.

The evidence that gun steels were indeed susceptible to stress corrosion when tested in a 3% NaCl solution led us to evaluate this

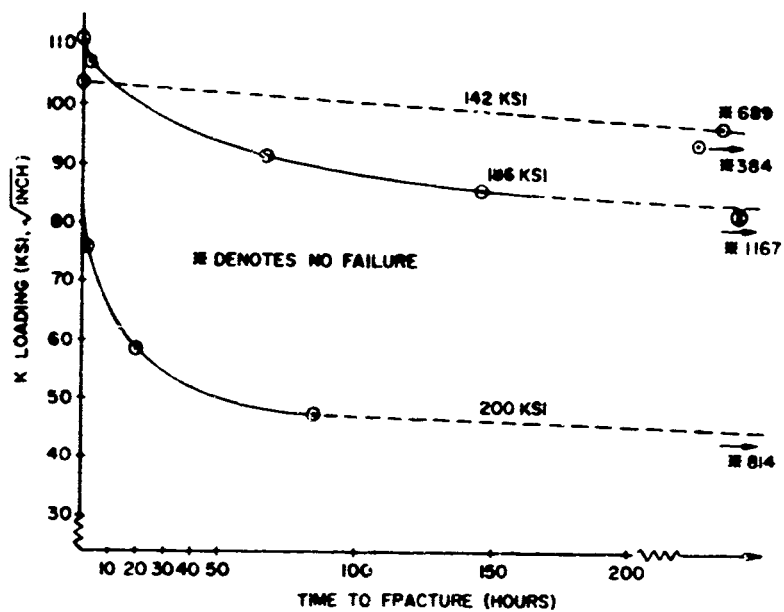


Figure 6. Effect of yield strength on fracture time, heat-treated tube 1100 in distilled H₂O.



Figure 7. Intergranular stress corrosion at crack tip of tube 7 in aqueous salt environment (1000X Nital Etch).

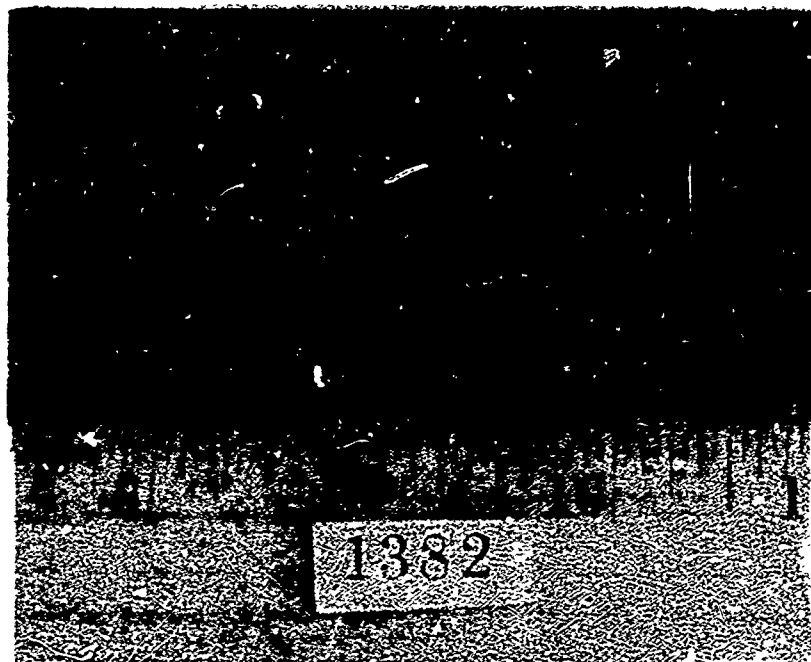


Figure 8. Macro photo of failure surfaces of gun tubes 1382 and 7, showing thumbnail corrosion markings.

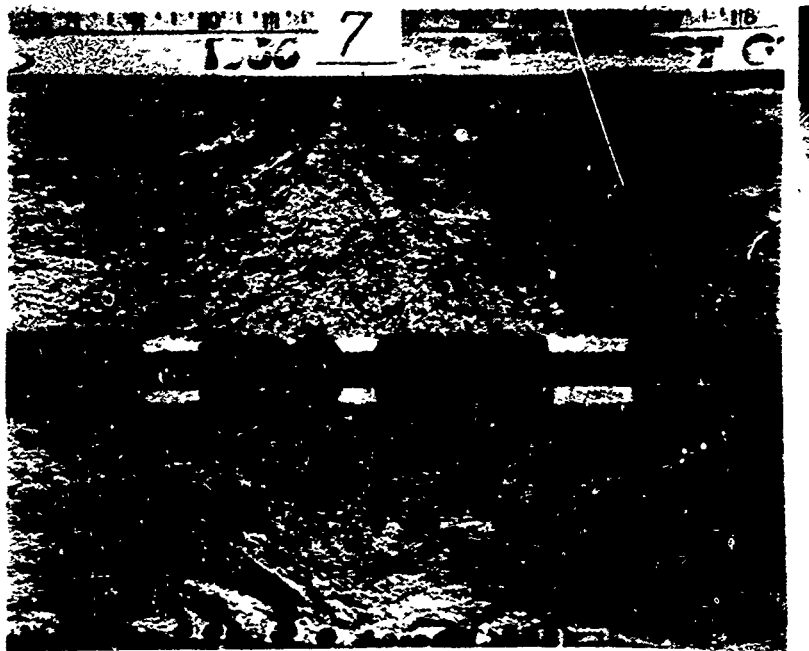


Figure 8. Continued.

susceptibility in other environments. Tube 7, which showed marked susceptibility in the NaCl solution, was used to evaluate the other environments. The data presented in table IV and figure 5 show that the distilled water and 100% RH air can also exert a degrading effect on the gun steel. For these tests, the water environment was slightly more damaging than the humid air, while the salt solution was considerably more damaging than either. The fact that gun steels can be degraded via stress corrosion damage by a compound as ubiquitous as water causes, first, concern, and secondly, speculation as to why evidence of stress corrosion is not more widespread. One can only comment that stress corrosion by definition requires the presence of significant stresses as well as a damaging environment and that corrosion is a time dependent phenomenon. Residual stresses of sufficient magnitude to cause damage to a normal tube (as compared with a temper embrittled tube) may not always be present. Secondly, if tubes are being fired rapidly, the lives are probably limited by fatigue, and time for the development of stress corrosion cracks would be limited. If, however, such stress corrosion damage did occur, it would permit crack extension without additional firing, thus distorting the cyclic base in fatigue studies.

Having determined the relative susceptibility in varying environments, the investigation was continued to determine whether variations in yield strength level would produce significant changes in the stress corrosion response. The results of tests conducted in distilled water are presented in table V and shown graphically in figure 6. It is

readily apparent that the K_{Isc} level is decreased markedly with increasing yield strength. The 142, 186 and 200 ksi YS materials exhibited K_{Isc} levels of 98, 85 and 45 ksi $\sqrt{\text{inch}}$ respectively in this environment. Examination of the fracture time vs. K_{Ii} curves leads one to speculate whether relative crack growth rates can be inferred. This would be desirable since it is difficult to rationalize the increase in failure times as being due solely to the increase in K_{Ic} values obtained when the yield strength was lowered. For example, from table V, if one compares the 186 ksi material ($K_{Ic} = 117 \text{ ksi } \sqrt{\text{inch}}$) loaded at an initial K level of 79.2 ksi $\sqrt{\text{inch}}$ with the 200 ksi material ($K_{Ic} = 96 \text{ ksi } \sqrt{\text{inch}}$) (loaded at a conservative initial K level of 58.1 ksi $\sqrt{\text{inch}}$), a decrease in fracture time of greater than 50 fold would be observed when going from the low yield strength to the high yield strength material. Stated differently, with the K_{Ii}/K_{Ic} ratio approximately the same, the 186 YS material has a life 50 times greater than the 200 YS material; consequently, there must be a difference in the crack growth rate.

This can be illustrated in the following manner. If a schematic crack depth vs. time curve is constructed, as in figure 9, critical crack depths pertinent to the relative yield strengths can be superimposed. For the 200 ksi material the crack progresses along line AB, with failure occurring at point B, corresponding to the critical crack depth (AC) at a failure time t_1 . For the 186 ksi material, assuming the same crack growth rate as in the prior case, the crack would continue along AB to point C, with the failure time denoted t_2 . One can

see that the increase in failure time ($t_2 - t_1$) is not a large value, and that increases in the order of fifty fold would not be obtained with reasonable increases in K_{IC} . For this reason, an adjunct experiment was conducted to determine crack growth rates. Since deflection vs. time curves were already available, deflection vs. crack depth curves were constructed for the various yield strength levels at various load levels as follows. Cantilever beam specimens of identical materials and strengths were stressed at the same dead weight loadings as those of the deflection vs. time curves previously obtained. Crack growth was simulated through physical extension of the crack front by means of a jeweler's saw blade. Micrometer readings of crack depth were plotted versus deflection readings obtained on the dial indicator. The calibration curve was produced at each load level so that deflection readings could be translated directly into crack depth values. Direct application of these values was made to obtain curves of crack depth vs. time in the corrosive environment. The curves obtained for 186 ksi and 200 ksi YS material at a single load level in the environment are shown in figure 10. The critical crack depths shown were calculated using approximate K_{IC} values from Wessels data on 4340⁴⁶, and assuming that rapid crack growth would occur when $K = K_{IC}$.

Examination of these curves shows that, in addition, to the deeper critical crack size in the lower yield material, the stress corrosion crack growth rate is slower. The action of both these factors results in a failure time which is considerably increased.

One can make a similar inference regarding crack growth rate in temper embrittled material by comparing times to failure; the data,

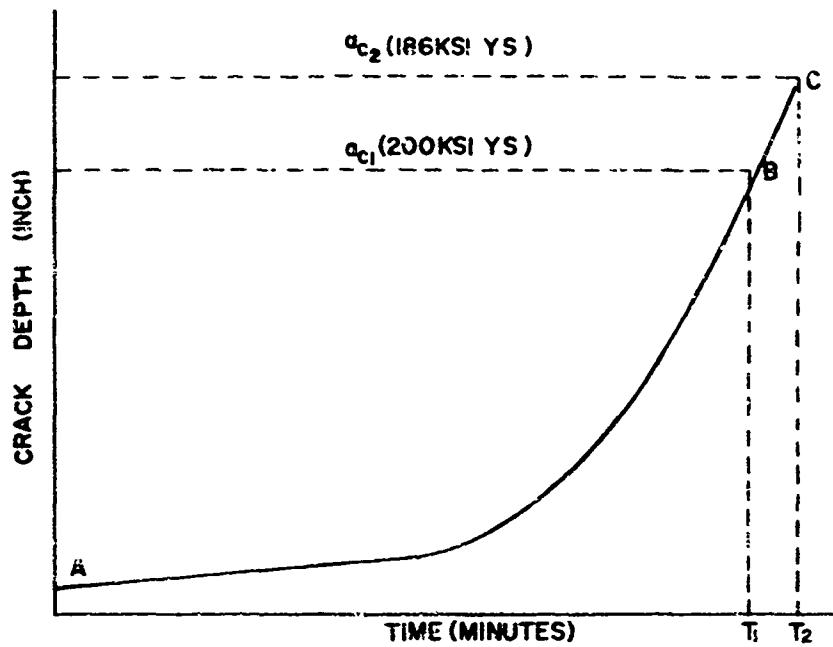


Figure 9. Curve illustrating effect of yield strength on crack growth.

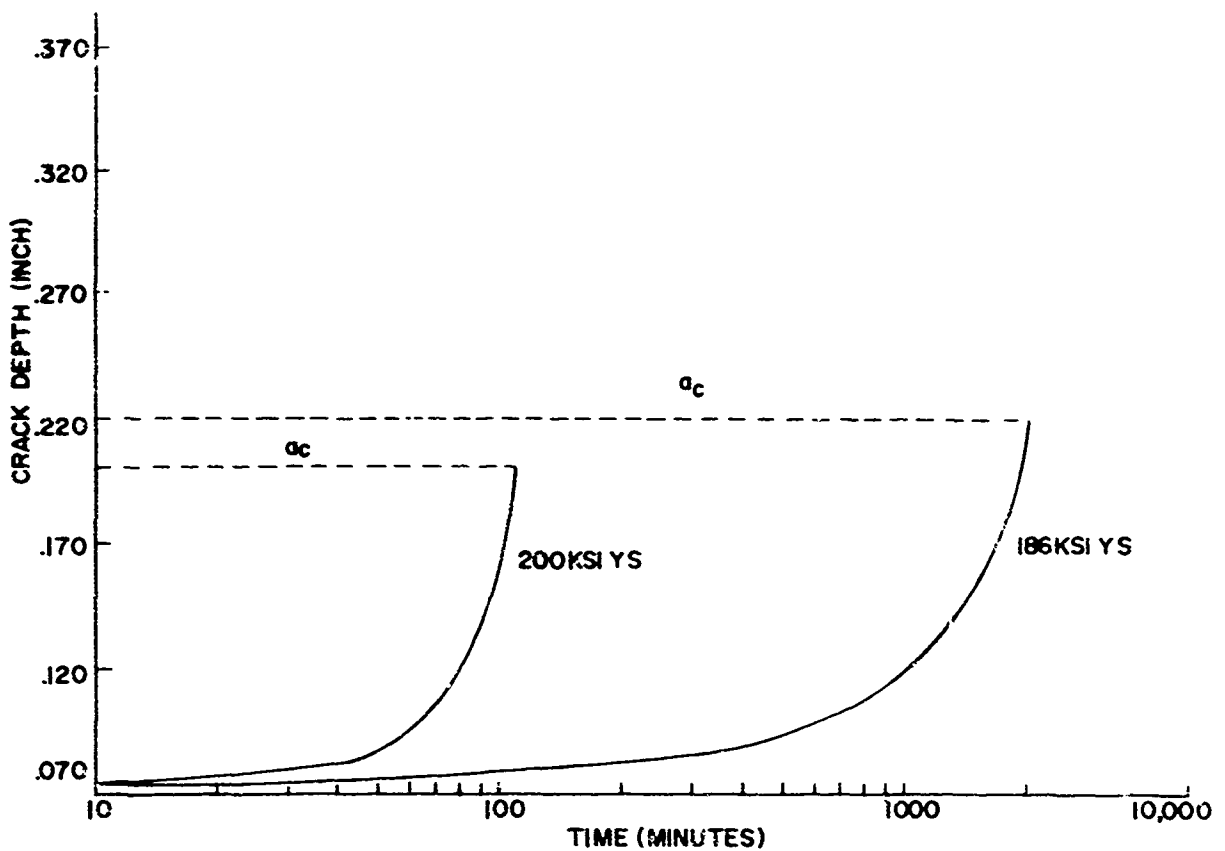


Figure 10. Effect of yield strength on crack growth - tube 1100 in 3% Na Cl- stress intensity factor of 50 ksi inch.

abstracted from table III, was obtained on specimens loaded to approximately the same K_{Ii} values.

<u>Tube</u>	<u>K_{Ic}</u>	<u>K_{Ii}</u>	<u>Time to Fracture</u>
7	117.5	48.1	13.6
1100	150	49.1	791 *

* Denotes no failure.

Note that tube 1100 exhibits a fracture time many times higher than tube 7, even though the initial loading was slightly higher. This increase in fracture time cannot be explained on the basis of a 25% increase in fracture toughness, even if one accepts the value of 150 ksi $\sqrt{\text{inch}}$ as being accurate.

Some comment should be made with respect to the mechanism of stress corrosion cracking in these high strength steels. The mode of failure was revealed by metallographic sectioning and electron microscope fractography to be intergranular in nature. Further, the fractograph shown in figure 11 shows that little destruction of the grain surfaces is occurring via dissolution. Such a result is incompatible with any theory of gross dissolution. The most likely mechanism is one of corrosion, followed by hydrogen embrittlement. The source of hydrogen is easily explained if one considers that in acidic or slight acidic solutions, hydrogen results as a corrosion product according to the following reaction:



The work of Johnson and Paris⁴⁷ has shown that crack growth rates can be markedly accelerated by the presence of hydrogen at the crack tip.

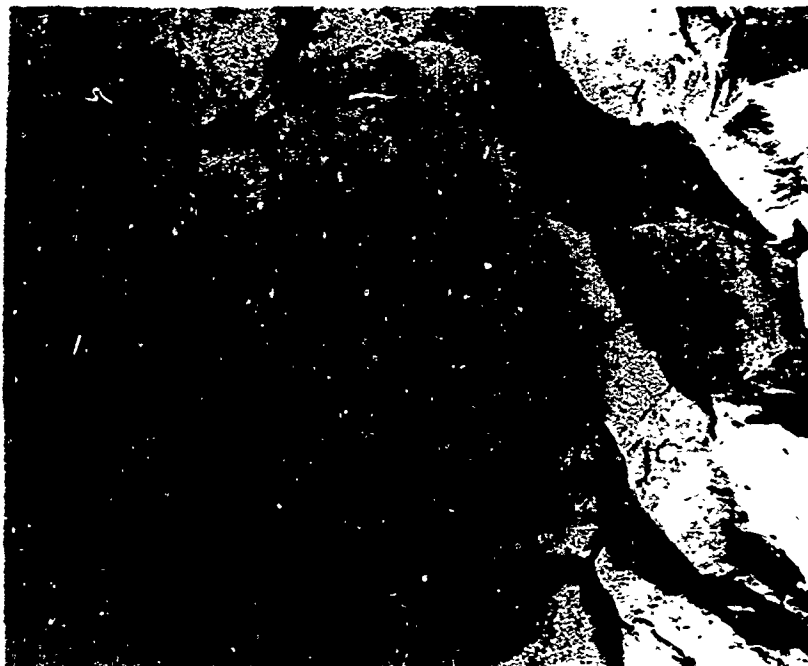


Figure II. Fractograph showing intergranular stress corrosion crack (3200X).

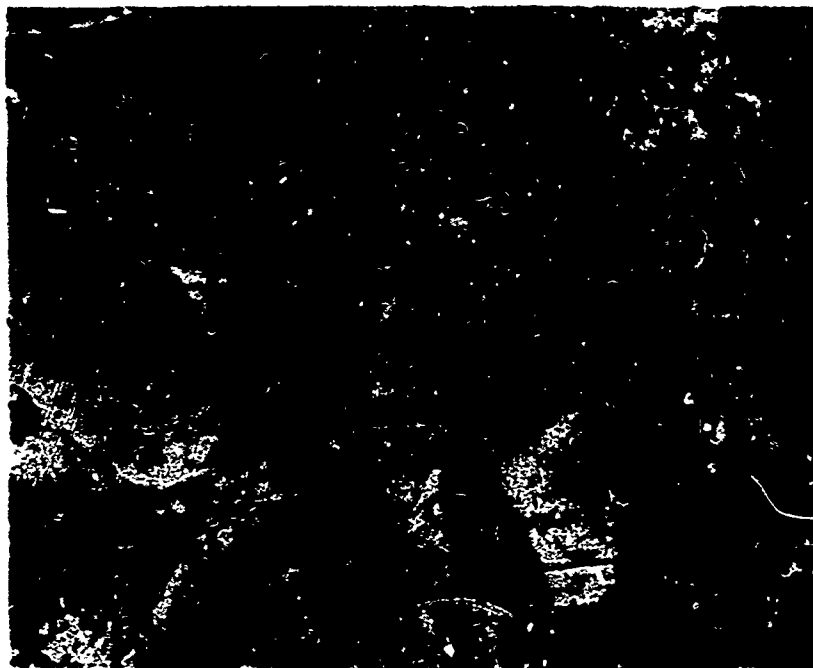


Figure 12. Fractograph showing H₂ charge brittle fracture (3200X).

Summarizing then, we have both an available source of hydrogen at the crack tip, and evidence that this hydrogen can exert a damaging influence. Of special interest is the fractograph shown in figure 12. This fractograph was produced from a tensile specimen which was deliberately hydrogen embrittled. Note the similarity between it and figure 11. In view of the previous discussion, such similarities appear more than coincidental, and provide additional proof that the hydrogen is largely responsible for the cracking process.

CONCLUSIONS

1. Failure times of gun steel specimens of the composition tested were related to the initial stress intensity level K_{Ii} . Increased K_{Ii} levels produced shorter failure times. The K_{ISCC} level was 55 ksi $\sqrt{\text{inch}}$ for all tubes except 7 and 1382 which exhibited a lower K_{ISCC} level of 35 ksi $\sqrt{\text{inch}}$. This reduction of the K_{ISCC} level below K_{IX} is conclusive evidence of the susceptibility of this gun steel to stress corrosion cracking. The K_{ISCC} being 65% below the K_{IX} level for tubes 7 and 1382 and 45% for the remainder of the tubes.

2. Stress corrosion damage in this material can occur in high humidity and water environments, though these are not as detrimental as a 3% NaCl solution. A decrease in fracture times was noted as environments were changed from 100% RH, to distilled water and to oxygenated 3% NaCl solution.

3. The apparent temper embrittlement of this composition tends to increase the stress corrosion susceptibility. Specimens from gun tubes tempered at approximately 900°F exhibited decreased failure

times when compared under identical conditions to tubes tempered at higher temperatures. This is manifested by a decrease in the K_{Isc} level from 55 ksi $\sqrt{\text{inch}}$ to 35 ksi $\sqrt{\text{inch}}$ for these tubes.

4. The increased stress corrosion susceptibility combined with the temper embrittlement appears to be detrimental to the actual fatigue life. Of the six tubes tested, tubes 7 and 1382 (temper embrittled) exhibited the lowest fatigue lives. Since this study was conducted, a third tube, 1144, of similar composition tempered at 915°F, with a life of 45.2 EFC rounds, has been tested and showed a similar decrease in fracture times.

5. Increasing yield strength from 142 ksi to 200 ksi produced an increasing susceptibility. The 142, 186 and 200 ksi YS materials exhibited K_{Isc} levels of 98, 85 and 45 ksi $\sqrt{\text{inch}}$, respectively, in distilled water. The decrease in fracture time was shown to be related to both a decrease in fracture toughness and an increase in the stress corrosion crack growth rate.

6. The mechanism advanced for the intergranular fracture observed is one of hydrogen embrittlement, in which the corrosion process provides the H_2 causing the embrittlement.

REFERENCES

1. Bechtol, H. A., Davidson, T. E., Bernstein, S. B., "Investigation of 175mm M113 Tube 733 Failure," U. S. Army Weapons Command Report (1 June 1966)
2. Davidson, T. E., Reiner, A. N., Throop, J. F., Nolan, C. J., "Fatigue and Fracture Analysis of the 175mm M113 Gun Tube," Watervliet Arsenal Report, WVT-6822 (November 1968)
3. Slawsky, M. L., Heiser, F. A., Liuzzi, L., "The Variation of Mechanical Properties in 175mm M113 Gun Tubes," Watervliet Arsenal Report, WVT-6734 (July 1967)
4. "Topical Discussion on Season and Corrosion Cracking of Brass," Proceedings, Am. Soc. Testing Matls., Vol. XVIII, Part II, pp. 147-219 (1918)
5. Newcomer, R., Tourkakis, H. C., Turner, H. C., "Elevated Temperature Stress Corrosion Resistance of Titanium Alloys," Corrosion, Vol. 21, #10, pp. 307-315 (October 1965)
6. Peterson, M. H., Brown, B. F., Newbegin, R. L., Groover, R. E., "Stress Corrosion Cracking of High Strength Steels and Titanium Alloys in Chloride Solutions at Ambient Temperatures," Corrosion, Vol. 23, #5, pp. 142-148 (May 1967)
7. Johnson, H. H. and Leja, J., "Surface Chemical Factors in the Stress-Corrosion Cracking of Alpha Brass," Corrosion, Vol. 22, #6, pp. 178-189 (June 1966)
8. Champion, F. A., "The Assessment of the Susceptibility of Aluminum Alloys to Stress Corrosion," Symposium on Stress Corrosion Cracking of Alloys, (STP64) ASTM, pp. 358-378 (1944)
9. Dean, S. W., Copson, H. R., "Stress Corrosion Behavior of Maraging Nickel Steels in Natural Environments," Corrosion, Vol. 21, #3, pp. 95-101 (March 1965)
10. Johnson, H. H. and Willner, A. M., "Moisture and Stable Crack Growth in a High Strength Steel", Applied Materials Research, Vol. 4, #1, pp. 34-40 (January 1965)
11. Van Der Sluys, W. A., "The Effect of Moisture on Slow Crack Growth in Thin Sheets of SAE 4340 Steel Under Static and Repeating Loading," Transactions of the ASME; Journal of Basic Engineering, pp. 28-34 (March 1967)

12. Henthorne, M., and Parkins, R. N., "Some Aspects of Stress - Corrosion Crack Propagation in Mild Steel," *Corrosion Science*, Volume 6, pp. 357-369 (1966)
13. Hancock, G. G. and Johnson, H. H., "Sub-Critical Crack Growth in AM 350 Steel," *Materials Research and Standards*, Vol. 6, No. 9, pp. 431-435 (September 1966)
14. Ibar, T. P., Hines, J. G., "The Stress-Corrosion Cracking of Austenitic Stainless Steels," *Journal Iron Steel Institute* 182, 124, (February 1956) and 182, 166 (October 1956) (2 part)
15. Hines, J. G., "Effect of Mechanical Factors on Corrosion," *Corrosion*, Vol. I, Ed. by L. L. Sheir, John Wiley and Sons, p. 8.3 (1963)
16. Parkins, R. N., "Stress Corrosion Cracking of Mild Steels," "Stress Corrosion Cracking and Embrittlement," (W. D. Robertson), Ed. Wiley, N. Y., pp. 140-157 (1956)
17. Copson, R. H., "Effect of Mechanical Factors on Corrosion," *The Corrosion Handbook*, H. H. Uhlig, John Wiley Sons, p. 569 (1948)
18. Dix, E. H., Jr., *Transactions, American Inst. Min. and Metall. Engr., Institute of Metals Division*, 137, p. 11 (1940)
19. Swann, P. R., and Pickering, H. W., "Implications of the Stress Aging Yield Phenomenon with Regard to Stress Corrosion Cracking," *Corrosion*, Vol. 19, No. 11, pp. 69t-372t (November 1963)
20. Forty, A. J., "The Initiation and Propagation of Cracks in the Stress Corrosion of Brass and Similar Alloys," in "Physical Metallurgy of Stress-Corrosion Fracture," Interscience, New York-London, pp. 99-116 (1959)
21. Hines, J. G. and Hugill, R. W., "Metallographic and Crystallographic Examination of S.C.C. in Austenitic Cr-Ni Steels", Forty, A. J., "The Initiation and Propagation of Cracks in the Stress Corrosion of Brass and Similar Alloys," in "Physical Metallurgy of Stress-Corrosion Fracture," Interscience, New York-London, pp. 193-226 (1959)
22. Graf, L., "Stress Corrosion Cracking in Homogeneous Alloys," Parkins, R. N., "Stress Corrosion Cracking of Mild Steels," "Stress Corrosion Cracking and Embrittlement," (W. D. Robertson), Ed. Wiley, N. Y., pp. 48-60 (1956)

23. Copson, H. R., "Effect of Composition on Stress Corrosion Cracking of Some Alloys Containing Nickel," Forty, A. J., "The Initiation and Propagation of Cracks in the Stress Corrosion of Brass and Similar Alloys," and "Physical Metallurgy of Stress-Corrosion Fracture," Interscience, New York-London, pp. 247-272 (1959)
24. Nielson, N. A., "The Role of Corrosion Products in Crack Propagation in Austenitic Stainless Steel Electron Microscopic Studies," Forty, A. J., "The Initiation and Propagation of Cracks in the Stress Corrosion of Brass and Similar Alloys," and "Physical Metallurgy of Stress-Corrosion Fracture," Interscience, New York-London, pp. 121-154 (1959)
25. Pickering, H. W., Beck, F. H., Fontana, M. G., "Wedging Action of Solid Corrosion Product During Stress Corrosion of Austenitic Stainless Steels," Corrosion, Vol. 18, pp. 230t - 239t (June 1962)
26. Keating, F. H., "Internal Stresses in Metals and Alloys," Institute of Metals, London, p. 311 (1948)
27. Evans, U. R., "Stress Corrosion; Its Relation to Other Types of Corrosion," Corrosion, Vol. 7, No. 7, pp. 238-244 (1959)
28. Parkins, R. N., "Caustic Cracking in Steam Boilers," Chemistry and Industry, pp. 180-184 (February 28, 1953)
29. Logan, H. L., "Film Rupture Mechanism of Stress Corrosion," Journal Research National Bureau of Standards, Vol. 48, No. 42, pp. 99-105 (February 1952)
30. Forty, A. J., "The Initiation and Propagation of Cracks in the Stress Corrosion of Brass and Similar Alloys," in "Physical Metallurgy of Stress-Corrosion Fracture," Interscience, New York-London, pp. 99-116 (1959)
31. Hines, J. G., "The Development of Stress Corrosion Cracks in Austenitic Cr-Ni Steels," Corrosion Science, Vol. 1, pp. 2-20 (1961)
32. Hines, J. G., "On the Propagation of Stress Corrosion Cracks in Metals," Corrosion Science, Vol. 1, pp. 21-48 (1961)
33. Barnett, W. J., Troiano, A. R., "Crack Propagation in the Hydrogen-Induced Brittle Fracture of Steel," Transactions AIME, Journal of Metals, pp. 486-494 (April 1957)
34. Kim, C. D. and Loginow, A. W., "Techniques for Investigating Hydrogen-Induced Cracking of Steels with High Yield Strength," Corrosion, Vol. 24, No. 10, pp. 313-318 (October 1968)

35. Evans, U. R., "On the Mechanism of Chemical Cracking," Parkins, R. N., "Stress Corrosion Cracking of Mild Steels," "Stress Corrosion Cracking and Embrittlement," (W. D. Robertson), Ed. Wiley, N. Y., pp. 158-162 (1956)
36. Brown, B. F., "Test Aids Stress Corrosion Research," The Iron Age, pp. 28-29 (November 21, 1968)
37. McEvily, A. J., Jr. and Bond, A. P., "On the Initiation and Growth of Stress Corrosion Cracks in Tarnished Brass," Journal Electric Society, 112, pp. 131-138 (February 2, 1965)
38. Logan, H. L., McBee, M. J., Kahan, D. J., "Evidence for an Electrochemical-Mechanical Stress-Corrosion Fracture in a Stainless Steel," Corrosion Science, Vol. 5, pp. 729-730 (1965)
39. Brown, B. F., "A New Stress Corrosion Cracking Test for High-Strength Alloys", Materials Research and Standards, Vol. 6, #3, pp. 129-133 (March 1966)
40. Bueckner, H. F., "The Propagation of Cracks and the Energy of Elastic Deformation," Transactions ASME, p. 1225-30 (August 1958)
41. Paris, P. C. and Sih, G. C., "Stress Analysis of Cracks," ASTM STP 381, pp. 30-83 (1965)
42. Kies, J. A., Smith, H. L., Romine, H. L., and Bernstein, H., "Fracture Testing of Weldments," Fracture Toughness Testing and Its Applications. ASTM STP 381, pp. 328-356 (1965)
43. Rolfe, S. T., Novak, S. R., and Gross, J. H., "Stress Corrosion Testing of Ultraservice Steels Using Fatigue-Cracked Specimens," U. S. Steel Corporation from ASTM Conference (June 1966)
44. Van Der Sluys, W. A., "Mechanisms of Environment Induced Sub-Critical Flaw Growth in AISI 4340 Steel," University of Illinois, Theoretical and Applied Mechanics Report No. 292 (September 1966)
45. Mulherin, J. H., "Stress Corrosion Susceptibility of High Strength Steel in Relation to Fracture Toughness," Transactions of the ASME, Journal of Basic Engineering, pp. 777-782 (December 1966)
46. Hays, L. E. and Wessel, E. T., "The Fracture Toughness of 4340 Steel at Various Yield Strength Levels, " Applied Materials Research (April 1963)
47. Johnson, H. H. and Paris, P. C., "Sub-Critical Flaw Growth," Engineering Fracture Mechanics, Vol. 1, No. 1 (June 1968)

Unclassified

Security Classification

DOCUMENT CONTROL DATA - R & D

(Security classification of title, body of abstract and indexing annotation must be entered when the overall report is classified)

1. ORIGINATING ACTIVITY (Corporate author) Watervliet Arsenal Watervliet, N.Y. 12189		2a. REPORT SECURITY CLASSIFICATION Unclassified	
		2b. GROUP	
3. REPORT TITLE SUSCEPTIBILITY OF GUN STEELS TO STRESS CORROSION CRACKING			
4. DESCRIPTIVE NOTES (Type of report and inclusive dates) Technical Report			
5. AUTHOR(S) (First name, middle initial, last name) Vito J. Colangelo Martin S. Ferguson			
6. REPORT DATE November 1970		7a. TOTAL NO. OF PAGES 42	7b. NO. OF REFS 47
8a. CONTRACT OR GRANT NO. AMCMS No. 4930.16.6661		9a. ORIGINATOR'S REPORT NUMBER(S) WVT-7012	
b. PROJECT NO. DA Project No. 66661			
c.		9b. OTHER REPORT NO(S) (Any other numbers that may be assigned this report)	
d.			
10. DISTRIBUTION STATEMENT This document has been approved for public release and sale; its distribution is unlimited.			
11. SUPPLEMENTARY NOTES		12. SPONSORING MILITARY ACTIVITY U.S. Army Weapons Command	
13. ABSTRACT Precracked cantilever beam specimens extracted from specific gun tubes were subjected to a constant load in various environments to determine fracture times. Specimens exhibited stress corrosion susceptibility in 3% NaCl, distilled water and 100% RH air, with 3% NaCl being the most degrading environment. Variations in susceptibility appeared on a tube to tube basis and were related to the temper embrittled condition of the tube. Additional tests in distilled water, varying yield strength material, showed that fracture time was decreased and crack growth rates increased as the yield strength was increased.			

DD FORM 1473
1 NOV 66REPLACES DD FORM 1473, 1 JAN 64, WHICH IS
OBSOLETE FOR ARMY USE.

Unclassified

Security Classification

Unclassified

Security Classification

14	KEY WORDS	LINK A		LINK B		LINK C	
		ROLE	WT	ROLE	WT	ROLE	WT
	Stress-corrosion						
	High strength steels						
	Hydrogen-embrittlement						
	Temper embrittlement						
	Precracked bend specimens						
	Fracture mechanics						

Unclassified

Security Classification